Lowland Technology International date; Volume 21 (Issue 2): 71-79
International Association of Lowland Technology (IALT): ISSN 1344-9656

Research Paper

Prediction of Uplift Capacity of Belled-type Pile with Shallow Foundation in Sandy Ground

J-G. Kang [1], N. Yasufuku [2], R. Ishikura [3], A. Y.Purnama [4]

ARTICLE INFORMATION

Article history:

Received: 3 January, 2019
Received in revised form: 21 April, 2019
Accepted: 3 July, 2019
Publish on: 5 September, 2019

Keywords:

Belled-type pile
Failure surface
Relative density
Pile tip inclination angle
Uplift load

ABSTRACT

This paper describes a semi-empirical model for predicting the uplift resistance of a belled-type pile considering the relative density of the ground. The variable parameters were utilized in the model are the pile length, the diameter of pile tip, the diameter of pile, and the angle of internal friction in the ground. Moreover, the inclination angle of pile tip and the relative density of the ground, which are not studied in the previous researches, were considered. In this study, an experimental model was conducted with various conditions such as the relative density of the ground and the inclination angle of pile tip those are designated to determine the failure surface of the ground. Based on results, a new model which can be applied to the belled-type pile was proposed by improving the limit equilibrium equation in the previous models. In addition, to confirm the reliability of the newly proposed a model of limit equilibrium equation of the belled-type pile, the models which are presented in the previous studies were compared with the proposed model. Consequently, the proposed model in this study correspond the higher reliability in comparison with the previous models.

1. Introduction

Generally, the pile foundation is designed to support the vertical loads of the superstructure. However, some special structures (e.g., high stacks, transmission towers, and coastal structures,) experience the horizontal load from wind, earthquake, tide, and waves that can induce lateral load and uplift load on the pile foundation. In the past 50 years, previous researchers have been developed a belled-type pile by modifying the pile tip with an anchor system (plate and pier, grillage, pedestal, pyramid, single and multi-helical anchor, grouted anchor, plate anchor, suction anchor) to increase the uplift resistance of pile foundation.

The belled-type pile can be effectively applied not only on the high stacks, transmission towers, and coastal structures but also for general structures. Though, the belled-type pile has a complicated mechanism causes influence of the pile tip shape, the belled-type piles have been widely applied large structures because of its ease of application in the field. Yet, there is a lack of clear mechanisms and design models that are reliable to apply on the field.

In this study, an experimental model was conducted on the belled-type pile with the different relative density of

[1] Jung-Goo Kang, Corresponding author. Ph.D. candidate, Department of Civil and Structural Engineering, Kyushu University. 744 Motooka Nishi-ku Fukuoka, 819-0395. TEL & FAX: (+81) 092802-3378; JAPAN, kang.junggoo.010@s.kyushu-u.ac.jp
[2] Noriyuki Yasufuku. Professor, Department of Civil and Structural Engineering, Kyushu University. 744 Motooka Nishi-ku Fukuoka, 819-0395. TEL: (+81) 092-802-3381; JAPAN, yasufuku@civil.kyushuu.ac.jp
[3] Ryohei Ishikura. Associate Professor, Department of Civil and Structural Engineering, Kyushu University. 744 Motooka Nishi-ku Fukuoka, 819-0395. TEL: (+81) 092-802-3382; JAPAN, ishikura@civil.kyushu-u.ac.jp
[4] Adhitya Yoga Purnama. Ph.D, Department of Civil and Structural Engineering, Kyushu University. 744 Motooka Nishi-ku Fukuoka, Japan, 819-0395. TEL & FAX: (+81) 092-802-3378; JAPAN, adhityayoga7@gmail.com
Note: Discussion on this paper is open until March 2020

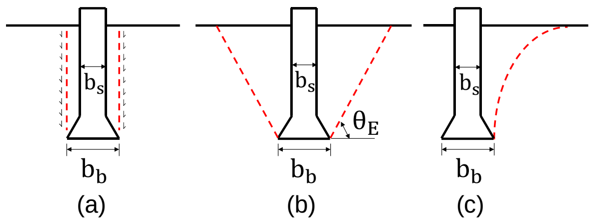

Fig. 1. Assumed failure mechanisms for belled piles subject to uplift loads.

ground soil and the inclination angle of pile tip which were not considered in the previous studies. Furthermore, a new design model which can be applied to the belled-type pile is proposed by improving the limit equilibrium equation of the previous models. Finally, the proposed model is compared with the previous models for evaluating the reliability of the proposed model.

The previous researches on uplift resistance of pile foundation had done for the transmission tower design. This study has been performed on a large field experiment. Generally, the evaluation of the uplift load on the pile is divided into two approaches. The first approach is based on surface friction between soil-pile (Meyerhof. 1973, Das. 1983).

The another one is based on the failure surface on the soil around the pile (Chattopadhyay and Pise. 1986, Shanker et al. 2007, Chim. 2013). However, the influence of various ground conditions and the geometrical characteristic of pile tip on belled-type are not clearly explained. In this study, the evaluation of belled-type pile by considering the failure surface was conducted to determine the influence of the pile tip shape on the uplift resistance.

Das (1986) classifies the failure mechanisms for the uplift loads into three types which are “The vertical slip model”, “The inverted truncated cone model”, and “The curved slip-surface model” as shown in Fig. 1.

Fig. 1 (a) shows the vertical slip model. The vertical slip model was proposed by Major (1955). This model was suggested that the weight of the belled-type pile, the weight of the soil on the sloped surface of the belled-type pile, and the shape of the base of the belled-type pile and the frictional resistance of the failure surface were generated in perpendicularly line due to uplift load.

Fig. 1 (b) shows the inverted truncated cone model. This model assumes that the frictional resistance of the failure surface generated as a cone shape from the end of the belled-type pile, until the ground surface. Herein, the previous researchers have presented various considerations about the failure angle (θ_E) generated from the pile tip. Mors (1959) assumes a truncated model is linear failure surface from the anchor tip to the ground surface, with the failure angle of 90°+φ. In addition, Downs and Chieurzi (1966) and Murray and Geddes (1987) are explained the angle of the failure surface (θ_E) was suggested to be the same as the internal friction angle (φ) of soil, while Clemence and Veesaert (1977) are suggested the failure angle as φ/2°. Sutherland et al. (1983) are suggested that the angle of inclination of the inverted truncated cone model surface is related to the internal friction angle of ground and ground density. It was also suggested that the shape of the failure surface changes depending on the density of ground.

Fig. 1 (c) shows the curved slip-surface model. The initial model was proposed by Balla’s (1961), which proposed a tangent curve for the failure surface of a mushroom-foundation. Meyerhof and Adams (1968) are used an experimental model to observe the slip surface of the pyramid-shape. In addition, Sutherland (1965) has confirmed that the shape of the failure surface was influenced by density of the ground and it concluded that Balla's (1961) analytical approach was only reliable at a specific density of ground.

Meyerhof and Adams (1968) observed $\varphi/4 < \theta_E < \varphi/2$ and taking an average value in the analysis. Also, previous researches have proposed a separate analysis of shallow and deep anchors. In addition, Sutherland et al. (1982) were simplified the theory of uplift resistance of anchors by considering the penetration depth. Matsuo (1967, 1968) has approached the failure surface with a logarithmic spiral and the tangent plane of 45°– φ/2° approach to the ground surface. Chattopadhyay and Pise (1985) has proposed a destructive surface using logarithm, assuming a normal pile. The model was compared with experimental model results.

2. Previous models

The following describes the previous uplift resistance equations for normal pile, belled-type pile and anchor plate.

2.1 Normal piles

Equation 1 shows the uplift resistance of the standard model. This equation is the most commonly used to estimate the uplift resistance by considering the pile-soil friction (φ/2°) and lateral earth pressure coefficient.

$$P_{u(net)} = \frac{\pi}{2} K_s b_b \gamma_d L^2 \tan\delta \quad [1]$$

Where, $P_{u(net)}$: Net ultimate uplift capacity, K_s: Coefficient of lateral earth pressure, b_b: belled-type pile tip diameter, γ_d: dry unit weight of sand, δ: pile-soil friction angle. The most important parameters in this equation are the lateral earth pressure coefficient and the pile-soil friction angle.

Das (2003) suggested the value of K_s for normal pile equal to $K_0 = K_s = (1–\sin\varphi)$.

Equation 2 represents the truncated cone model. This model is most commonly used in the field because it uses internal friction angles as a key parameter.

$$P_{u(net)} = \frac{\pi}{3} L^3 \tan^2 \frac{\varphi}{2} \gamma_d \qquad [2]$$

Where, $P_{u(net)}$: Net ultimate uplift capacity, φ: internal friction angle, L: penetration depth of pile, γ_d: dry unit weight.

2.2 Belled-type pile and anchor plate

Equation 3 is an equation based on the experimental model using anchor plates. This model was proposed by Meyerhof (1973) and it uses the uplift factor (K_u) from the model test results. Moreover, the model test results show that the failure surface is similar to the pyramid shape.

$$P_u = \gamma_d A_b L^2 \left(\frac{L}{b_b}\right) K_u \tan\varphi \left[m\left(\frac{L}{b_b}\right) + 1\right] + 1 \qquad [3]$$

Where, K_u: coefficient of uplift factor, m: pile tip shape factor, L: penetration depth of pile, A_b: belled-type pile tip area, b_b: belled-type pile tip diameter, φ: internal friction angle, γ_d: dry unit weight.

Equation 4 was proposed by the model test results of Downs and Chieurzzi (1966). The calculation was proposed by considering the effect of the pile tip diameter and pile column diameter.

$$P_u = \gamma_d A_b L^2 \left(\frac{L}{b_b}\right) K_u \tan\varphi \left[m\left(\frac{L}{b_b}\right) + 1\right] + 1 \qquad [4]$$

Where, L: penetration depth of pile, b_b: belled-type pile tip diameter, b_s: pile column diameter, φ: internal friction angle, γ_d: dry unit weight.

Equation 5 is proposed by Ovesen (1981) using the results of centrifugal model experiments. In this experiment, an uplift load was applied on the anchor plate pile and a reliable failure surface was obtained. Where bb is the tip diameter and be is the corrected diameter.

$$P_u = \gamma_d A_b L \left(1 + (4.32 \times \tan\varphi - 1.58)\left(\frac{L}{b_e}\right)^{1.5}\right), b_e = \sqrt{\frac{\pi {b_b}^2}{4}} \qquad [5]$$

Where, K_u: coefficient of uplift factor, b_e: pile tip shape factor, L: penetration depth of pile, A_b: belled-type pile tip area, b_b: belled-type pile tip diameter, φ: internal friction angle, γ_d: dry unit weight.

Balla's (1961) proposed an estimation equation model by assuming the shear plane of the small model anchor is tangent-curved (**Equation 6**). According to Balla's model, the failure surface of the pile embedded in dense sand was a circular curve from the end of pile tip to the ground and the failure angle was approximately 45º– φ/2°. It assumed the failure surface was circular and the circular failure surface of the foundation using various scale experiments on shallow foundations.

$$P_u = \gamma_d A_b L \left[(F_1 + F_3)\left(\frac{4}{\pi}\right)\left(\frac{L}{b_b}\right)^2\right] \qquad [6\text{-a}]$$

$$F_1 + F_3 = -0.0171\left(\frac{L}{b_b}\right)^3 + 0.3057\left(\frac{L}{b_b}\right)^2 - 1.7937\left(\frac{L}{b_b}\right) + 4.0389 \qquad [6\text{-b}]$$

F1 and F3 are functions of the peak friction angle which are obtained from the chart proposed by Balla's (1961). **Equation 6-a** shows the relationship between F1 and F3. Where, γ_d: dry unit weight of sand, A_b: belled-type pile tip area, L: penetration depth of pile, b_b: belled-type pile tip diameter.

3. The proposal models

The proposed model is developed by considering the tip inclination angle of the belled-type pile. Moreover, the failure surface proposed in this study was assumed as linear and the failure shape follows, the inverted cone model. The new model was proposed by improving the previous research models (Das.1983, Kang.2016) based on the limit equilibrium method of the normal pile.

3.1 Failure surface and failure angle

Fig.2 shows the shape of the failure surface of the belled-type pile identified in previous studies (Kang. 2016). It is difficult to clearly determine the difference between the linear and nonlinear failure surface of the ground soil obtained from the model experiment results. Therefore, in this research, in order to simplify the calculation, the failure surface was assumed to be a linear line.

In the previous research of uplift loading on the normal pile, the value of the failure angle, is equal to φ/4 (Shanker et al. 2007), which has similar value with the experimental results. In addition, Das (1983) had investigated by using the model experiment and concluded that the uplift load decreases depend on the penetration depth and sand relative density (Dr = 70%) (**Equation 8**). According to the results, the coefficient of density was proposed (κ). This coefficient was determined based on experimental results. The following

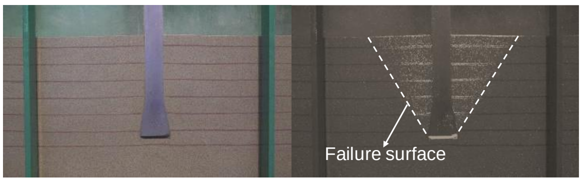

Fig.2. A Study on the Failure Surface of Bell Type Pile Model Test Using Image Analysis.

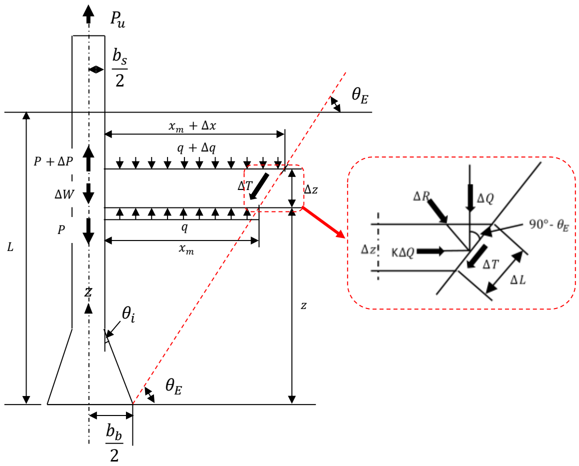

Fig. 3. A Study on the failure surface of belled-type pile model experiment using image analysis

failure angles were estimated based on the results of the above two studies and the pile tip inclination angle as following **Equation 7**.

$$\theta_E = \left(90° - \frac{\psi}{2} - \theta_i\right) \times \kappa \qquad [7]$$

$$\kappa = \left(1 - \frac{Dr}{100} + 0.7\right) \qquad [8]$$

Where, κ: Coefficient of unit weight, Dr: Relative density (%), ψ: Dilatancy angle (φ/2°, φ –30°), φ: Internal friction angle (°), θ_E: Failure angle (°).

3.2 Uplift load model

The proposed model was analyzed based on the limit equilibrium equations of Chattopadhyay and Pise (1986). Chattopadhyay and Pise (1986) conducted a model experiment on the uplift load on the normal pile and the model was presented using the limit equilibrium method. In addition, this study has compared the results of the model experiment with the proposed models. In the research by Chattopadhyay and Pise (1986), the failure surfaces were evaluated by considering the pile tip inclination angle to simplify the failure surface, assuming the failure plane is linear line. In the proposed model of the failure surface, the pile tip inclination angle was considered. Which was not considered in the previous researches. The proposed model assumes the following three assumptions.

1) The failure surface intersects linearly with the surface of the ground.
2) For a belled-type pile with $\delta \geq 0$, the angle between the failure surface and the surface is assumed to approach **Equation 7** based on the previous researches. κ means the coefficient assumed in the previous researches.
3) For piles with $\delta \geq 0$, subject to ultimate uplift force P_u, the failure surface starts tangentially to the ground surface. Shear resistance (ΔT) along the failure surface length (ΔH) can be calculated by the following equation

Thus:

$$\Delta R = \Delta Q(\cos\theta_E + K_0 \sin\theta_E) \qquad [9]$$

Where:

$$K = K_0(1 - \sin\varphi) \qquad [10]$$

In Fig. 3, ΔQ can be expressed as follows.

$$\Delta Q = \gamma_d(L - z - \Delta z/2)/\Delta L \qquad [11]$$

$$\Delta L = \frac{\Delta z}{\sin\theta_E} \qquad [12]$$

Where:

$$\Delta R = \gamma_d\left(L - z - \frac{\Delta z}{2}\right)(\cos\theta_E + K_0\sin\theta_E)\frac{\Delta z}{\sin\theta_E} \qquad [13]$$

and

$$\Delta T = \gamma_d\left(L - z - \frac{\Delta z}{2}\right)(\cos\theta_E + K_0\sin\theta_E)\frac{\Delta z}{\sin\theta_E}\tan\varphi \qquad [14]$$

Considering the vertical equilibrium of the circular wedge and assuming that the weight of the pile of length dz equals the weight of the pile to the volume occupied by the pile.

$$(P + \Delta P) - P + q\pi x_m^2 - (q + \Delta q)\pi(x_m^2 + \Delta x)^2 - \Delta W - 2\pi\left(x_m^2 + \frac{\Delta x}{2}\right)\Delta T \sin\theta_E = 0 \qquad [15]$$

Equation 15 replaces and simplifies the value from **Equation 16**.

$$\frac{\Delta P}{\Delta z} = \pi q \frac{\Delta x}{\Delta z}(2x_m + \Delta x) + \pi\frac{\Delta q}{\Delta z}(x_m + \Delta x)^2 + \pi\frac{\Delta q}{\Delta z}(x_m + \Delta x)^2 + \pi(x_m + \Delta x)^2\gamma_d + 2\pi\left(x_m + \frac{\Delta x}{x}\right)\gamma_d\left(L - z - \frac{\Delta z}{2}\right)(\cos\theta_E + K_0\sin\theta_E)\tan\varphi \qquad [16]$$

At the limit, to replace *q* in Eq.16 with q = γ_d (L - z).

$$\frac{dP}{dz} = 2\pi\left(\frac{z}{\tan\theta_E} + \frac{b_b}{2}\right)\gamma_d(L - z)\frac{1}{\tan\theta_E} + 2\pi\left(\frac{z}{\tan\theta_E} + \frac{b_b}{2}\right)\gamma_d(L - z)(\cos\theta_E + K_0\sin\theta_E)\tan\varphi \qquad [17]$$

Eq.17 as an integral, it was organized as Eq.18.

$$P_u = \int_0^L 2\pi\left(\frac{z}{\tan\theta_E} + \frac{b_b}{2}\right)\gamma_d(L - z)\left[\frac{1}{\tan\theta_E} + (\cos\theta_E + K_0\sin\theta_E)\tan\varphi\right]dz \qquad [18]$$

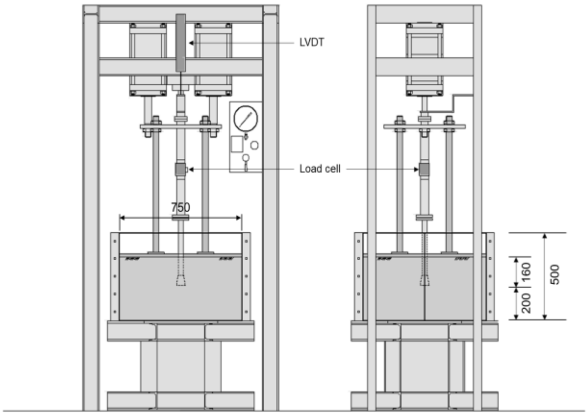

Fig. 4. Model experiment apparatus

If except the weight of the pile, it can be expressed as follows. Herein, the shape of the pile is assumed to be a normal pile for simple calculation.

$$P_{u(net)} = P_u - \frac{\pi b_b^{\,2}}{4} \times L \times \gamma_d \qquad [19]$$

4. Expermental model test

Fig. 4 shows a schematic diagram of the experimental model performed in the laboratory. The model circle chamber diameter is 500mm in height and 750 mm in diameter. In addition, the inside of the model chamber (Fig. 5) is coated with a Teflon, which minimizes the friction that can occur between the soil and the chamber.

Table. 1 shows the model experimental conditions. In order to investigate the influence of the relative density and the tip shape of the belled-type pile, the model experiments were carried out under the conditions of three different pile tip inclination angle (θ_i = 0°, 12°, 18°) and five different relative density (Dr = 40%, 60%, 75%, 85%, 95%).

Table. 1. Model experiment conditions

Descriptions		Experimental adjustments
Inclination angle of pile tip	(°)	0, 12, 18
Unit weight	(%)	40, 60, 75, 85, 95
Penetration depth	(mm)	160
Penetration ratio		3.33

Fig. 5. Model chamber

Fig. 6 and Table. 2 show the results of particle size distribution and physical properties of the soil used in the experiment. The soil was classified as silty sand (SM) based on the USCS classification system. In the model experiment, the penetration depth of belled-type pile was 16cm, which was classified as a shallow foundation based on the pile slenderness ratio (L/b_b <4). The uplift loading was applied on the pile head by controlling the strain rate using the screw jaw. In this research, the experiment was carried out with the minimum loading rate of 4mm/min for the accuracy of the result.

5. Results and Discussion

The representative uplift load models in previous researches and experimental results in this research were compared. In the selection of representative models in the previous researches, typical models using normal piles, belled-type piles, and anchor plates were selected.

In the selection of representative models, which are

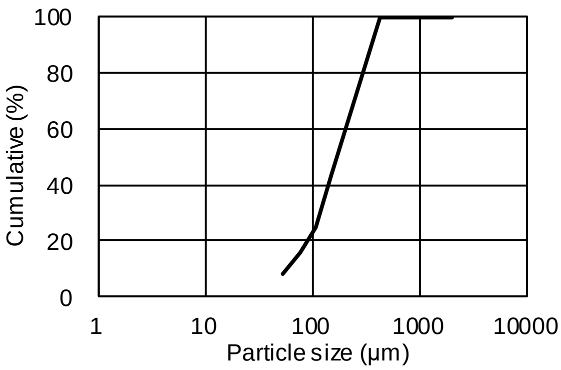

Fig. 6. Particle size distribution curve (USCS)

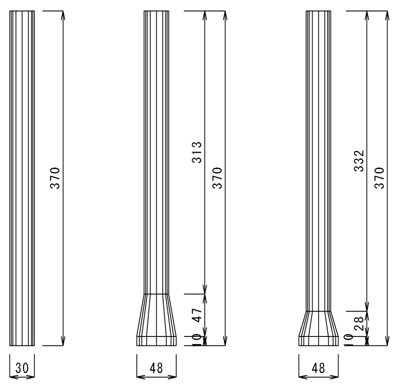

Fig. 7. Model pile

Table. 2. Physical properties of weathered granite soil

Property		Value
Liquid limit, LL	(%)	N.P
Plastic limit, PL	(%)	N.P
Specific gravity, G_s		2.63
Fine-grained soil	(%)	15.6
Unified Soil Classification System (USCS)		SM
Maximum density, ρ_{max}	(g/cm^3)	1.571
Minimum density, ρ_{min}	(g/cm^3)	1.197
Internal friction angle	(°)	42 (Dr = 80%)

similar with parameter characteristics such as internal friction angle and relative density were selected, respectively. Moreover, in order to compare quantitatively the calculated results of the previous models with the proposed model results, the percentage of error was evaluated.

Equation 20 represents the difference between the calculation result the model experiment result as an absolute value in percentage.

$$\varepsilon\,(\%) = \left|\frac{(P_u)_{predicted} - (P_u)_{experiment}}{(P_u)_{experiment}}\right| \times 100 \qquad [20]$$

5.1 Model experiment results

Fig. 8 shows the result of experimental model. Experimental model was conducted to confirm the effect of the ground and the tip inclination angle of the belled pile. The uplift load of a normal pile was measured as a comparison with the uplift load of a belled-type pile.

Based on Fig. 8 (a), the uplift load of a normal pile is lower than belled-type pile. In addition, the higher uplift load was confirmed in the relative density of 85% or more.

This result has been suggested about not only the pile-soil friction but also the failure surface occurred at the same time. Fig. 8 (b, c) show the uplift loading results of the belled-type pile. In the model experiment with two different inclination angles of belled-type piles (θ_i = 12°, 18°), the peak value of uplift load was not confirmed in the experiment with the relative density of 40%. This result was indicated that the compaction was occurred above of the belled part in case of low density. Consequently, the effect of uplift load in belled-type pile is insignificant, which was confirmed in the previous researches (Lin, 2015).

Furthermore, in case of relative density of 60% or more, which was indicated that the influence of the failure surface and the pile-soil friction were occurred at the relative density which was relatively lower than the case of the normal pile causes the influence of the belled-type pile tip.

Table. 3 shows the maximum value of the uplift loading. In this experiment, the maximum uplift loading was confirmed under the condition of the tip inclination angle of 12° and the relative density of 95%. This value is 10 times higher than the condition of relative density of 40% with the same tip inclination angle of 12°. In addition, the result of inclination angle of the pile tip shows that the uplift loading on $\theta_i = 12°$ is slightly higher than the result of $\theta_i = 18°$.

5.2 Comparison of model experiment results and previous models

Table. 3 and Fig. 9 show the calculation results of the previous models and the experimental results of the model experiments. Fig. 10 shows the internal friction

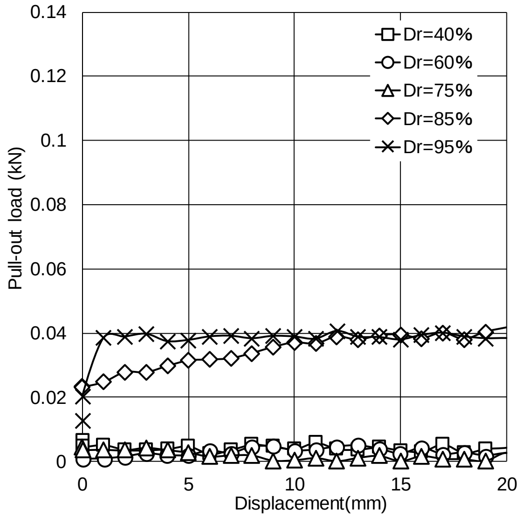

(a) $\theta_i = 0°$

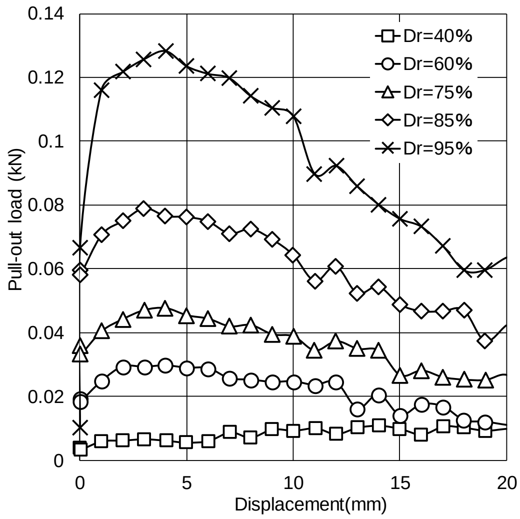

(b) $\theta_i = 12°$

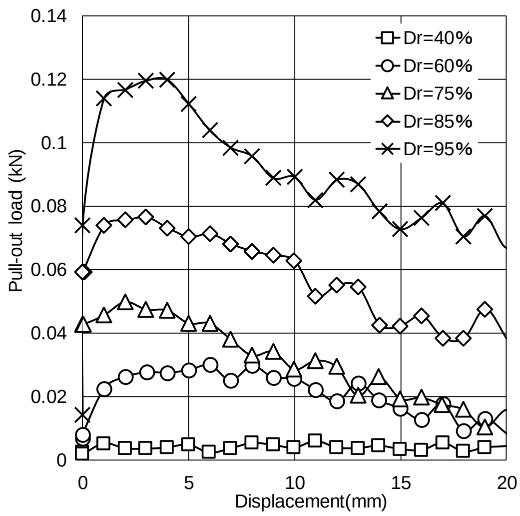

(c) $\theta_i = 18°$

Fig. 8. The results of an uplift load for normal and belled-type piles

Table. 3. Comparison of model test results with previous models

Inclination angle θ_i(°)	Unit weight %	Unit volume (kN/m3)	Internal friction angle φ(°)	Standard model Pu(kN)	Standard model ε(%)	Truncated cone model Pu(kN)	Truncated cone model ε(%)	Meyerhof's model Pu(kN)	Meyerhof's model ε(%)	Downs and Chieurzzi Pu(kN)	Downs and Chieurzzi ε(%)	Ovesen Pu(kN)	Ovesen ε(%)	Balla Pu(kN)	Balla ε(%)	Experiment Pu(kN)
0	40	13.13	35.0	0.002	228.7	0.006	25.0	0.012	42.8	0.021	66.2	0.033	78.9	0.004	57.6	0.007
	65	13.88	38.5	0.002	262.5	0.007	10.2	0.016	51.2	0.026	69.4	0.045	82.1	0.005	69.8	0.008
	75	14.44	41.1	0.002	213.0	0.009	19.7	0.021	66.2	0.031	77.6	0.054	87.1	0.005	43.3	0.007
	85	14.81	42.9	0.002	1817.7	0.010	339.0	0.024	76.6	0.035	22.5	0.062	30.4	0.005	761.9	0.043
	95	15.19	44.6	0.002	1777.6	0.011	282.9	0.029	45.9	0.040	6.3	0.070	39.8	0.005	726.8	0.042
12	40	13.13	35.0	0.003	252.2	0.006	114.3	0.031	61.7	0.051	76.3	0.044	72.6	0.011	5.6	0.012
	65	13.88	38.5	0.004	806.3	0.007	340.8	0.042	23.8	0.065	50.4	0.058	45.2	0.012	165.3	0.032
	75	14.44	41.1	0.004	1241.4	0.009	450.8	0.053	9.4	0.077	37.9	0.071	32.4	0.013	283.7	0.048
	85	14.81	42.9	0.004	2157.7	0.010	727.0	0.062	30.0	0.087	7.2	0.080	0.8	0.013	534.2	0.081
	95	15.19	44.6	0.004	3532.3	0.011	1085.1	0.074	76.4	0.098	32.0	0.090	43.7	0.013	899.7	0.13
18	40	13.13	35.0	0.003	105.4	0.006	25.0	0.031	77.7	0.051	86.2	0.044	84.0	0.011	38.4	0.007
	65	13.88	38.5	0.004	777.9	0.007	327.1	0.042	26.2	0.065	52.0	0.058	46.9	0.012	157.0	0.031
	75	14.44	41.1	0.004	906.0	0.009	313.1	0.053	32.1	0.077	53.5	0.071	49.3	0.013	187.8	0.036
	85	14.81	42.9	0.004	2074.1	0.010	696.3	0.062	25.2	0.087	10.6	0.080	2.9	0.013	510.7	0.078
	95	15.19	44.6	0.004	3308.8	0.011	1012.1	0.074	65.5	0.098	23.9	0.090	34.9	0.013	838.2	0.122

angle with different relative density. The dilatancy angle (ψ) and the pile-soil friction angle (δ) used in the model calculations were provided in the reference ($\delta = \psi = \varphi/2$). In addition, since the tip diameters (b_b = 0.048 m) of the belled-type piles used in this research were the same, the calculation results of the two types of belled-type piles ($\theta_i = 12°$, 18°) were the same.

In case of the normal pile ($\theta_i = 0°$), the standard model (**Equation 1**) has shown a difference of uplift loading of up to 17 times (Dr = 95%) depending on the relative density. Based on the result of the comparison of the truncated cone model, a difference of up to 3 times was confirmed depending on the relative density of 85%. For the truncated cone model, the results of highly reliable experiments were confirmed under the conditions of relative density of 75% or less.

It can be concluded that the reliability of the proposed model is higher than the normal pile model ($\theta_i = 0°$). The models of Meyerhof's (1973), Downs and Chieurzzi's (1966) have shown relatively good corresponding. Comparing to Meyerhof's model, Downs and Chieurzzi's (1966) and Ovesen (1981), the reliability of the model test results of the belled-type pile was higher than the other models. In the other models, the percentage of error was more than 100%.

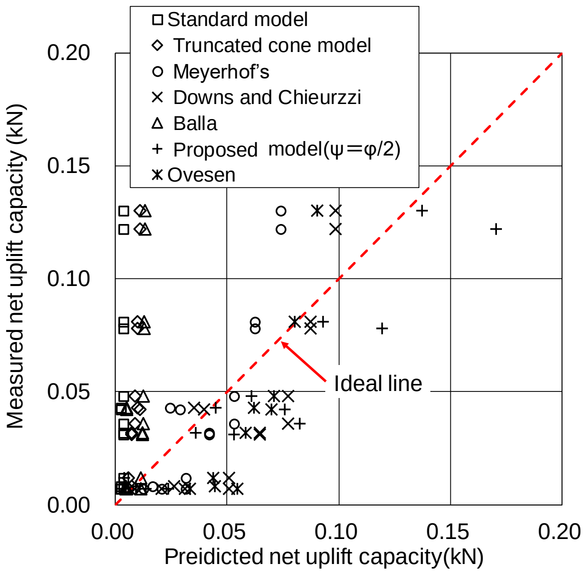

Fig. 9. Comparison between the proposed model and the previous models

5.3 Influence of dilatancy angle on the proposed model

Generally, the dilatancy angle relates to the volumetric deformation rate of the ground, therefore a complex experiment is required. Previous researchers have studied the relationship between internal friction angle and dilatancy angle using model experiments (Das. 1983, Japan Geotechnical Society. 1995) and are currently using the results extensively.

In this research, the dilatancy angle was used as an important parameter to determine the failure angle (θ_E).

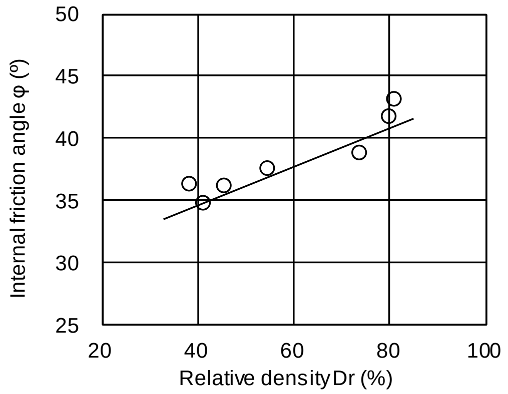

Fig. 10. Direct shear test on relative density

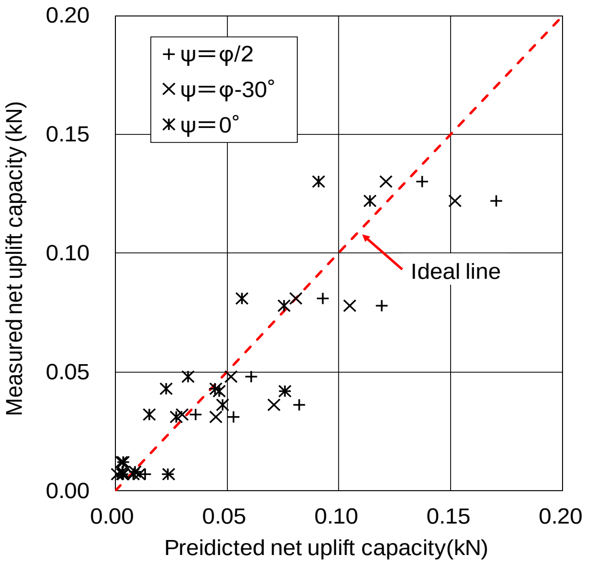

Fig. 11. Comparison of the dilatancy angle (ψ)

Table. 4. The calculation and comparison of the proposed models for dilatancy angle (ψ)

Inclination angle	Unit weight	Unit volume	Internal friction angle	The proposed model						Experiment
				ψ = 0°		ψ = φ/2		ψ = φ-30°		
θ_i(°)	%	(kN/m^3)	φ(°)	Pu(kN)	ε(%)	Pu(kN)	ε(%)	Pu(kN)	ε(%)	Pu(kN)
0	40	13.13	35.0	0.0032	115.7	0.003	115.7	0.001	600.0	0.007
	65	13.88	38.5	0.0035	131.3	0.009	12.6	0.009	11.1	0.008
	75	14.44	41.1	0.0083	15.6	0.024	70.3	0.024	70.8	0.007
	85	14.81	42.9	0.0230	86.9	0.045	3.9	0.045	4.4	0.043
	95	15.19	44.6	0.0465	9.6	0.076	44.7	0.076	44.7	0.042
12	40	13.13	35.0	0.0038	218.7	0.004	218.7	0.003	300.0	0.012
	65	13.88	38.5	0.0154	107.3	0.036	11.1	0.03	6.7	0.032
	75	14.44	41.1	0.0328	46.5	0.061	21.1	0.052	7.7	0.048
	85	14.81	42.9	0.0569	42.3	0.093	12.8	0.081	0.0	0.081
	95	15.19	44.6	0.0911	42.7	0.137	5.4	0.121	7.4	0.13
18	40	13.13	35.0	0.0038	85.9	0.014	48.6	0.011	36.4	0.007
	65	13.88	38.5	0.0273	13.4	0.053	41.6	0.045	31.1	0.031
	75	14.44	41.1	0.0480	24.9	0.082	56.3	0.071	49.3	0.036
	85	14.81	42.9	0.0755	3.2	0.119	34.6	0.105	25.7	0.078
	95	15.19	44.6	0.1140	7.0	0.170	28.4	0.152	19.7	0.122

Therefore, the proposed model was compared using two different dilatancy angles ($\psi = \varphi/2°$, $\psi = \varphi - 30°$). Fig. 11 and Table. 4 show the comparison between the calculated values of the proposed model for two dilatancy angles and the uplift loading of model tests. The calculated values with dilatancy angle of $\psi = \varphi/2°$ was about 16% higher than the experimental values. In addition, in the Table. 4, the error was found 50% or less in most cases excluding the case with relative density of 40%.

In the predicted result with dilatancy angle of $\psi = \varphi - 30°$, an error was smaller than the result with dilatancy of $\psi = \varphi/2°$. Particularly, in the case of the belled-type pile with pile tip inclination angle of 12°, the error was less than 10% excluding the case with relative density of 40%, and the reliability was found very high. However, the calculation results with dilatancy angle of $\psi = \varphi - 30°$ of 40% of relative density, the pile tip inclination angle of 0° and 12° were calculated much lower than the experimental value.

6. Conclusion

In this research, a new uplift resistance model of belled-type pile was proposed using the equilibrium equation. The experimental model was performed to confirm the reliability of the proposed model by considering the inclination angle of pile tip of belled-type piles and relative densities of ground. The conclusion of this research can be summarized as follows:

(1) The effect of load resistance in belled-type piles were not significant in case of ground with 40% of relative density in both piles with inclination angles. This result was similar to the previous researches and it seems that the compaction on the pile tip area was occurred. In the result, where was not influence of pile tip shape on the uplift capacity on the low density in ground. In addition, the uplift capacity of belled-type pile with pile inclination angle of 12° is slightly higher than the 18° of pile inclination angle.

(2) The standard model and the truncated cone model generate the higher difference value of predicted uplift capacity compared to the experimental results. It was indicated about 33 times difference between experimental and predicted model. The proposed model corresponding better accuracy than the previous models to predict the uplift capacity of the normal pile embedded into different ground density.

(3) A new equation model considering the characteristics of belled-type piles was proposed by using the limit equilibrium method. The dilatancy angle of the ground was considered as a key parameter to predict the uplift capacity of belled-type pile. The dilatancy angle value of $\psi = \varphi - 30°$ provide the lowest average error to predict the uplift capacity. The result has been shown that the maximum error of the proposed model in the belled-type pile was less than 50%, excluding the case with relative density of 40%.

Reference

B. C. Chattopadhyay. and P. J. Pise., 1986. Uplift Capacity of Piles in Sand. Journal of Geotechnical Engineering, **51** (3): 888-904.

Braja. M. Das., 1978. Model tests for uplift capacity of foundations in clay. Soils and Foundations, **18** (2): 17-24.

Braja. M. Das., 1983. A procedure for estimation of uplift capacity of rough piles. Soils and Foundations, **23** (3): 122-126.

Braja, M, D., Gerald. R. S, and Thomas. W. P, 1997. Pullout resistance of rough rigid piles in granular soil. Soils and Foundations, **17** (3): 72-77.

E. A. Dickin. And C. F. Leung., 1990. Performance of piles with enlarged bases subject to uplift forces. Canadian Geotechnical Journal, **27** (5): 546-556.

E. A. Dickn. and C. F. Leung., 1992. The influence of foundation geometry on the uplift behaviour of piles with enlarged bases. Canadian Geotechnical Journal, **29** (3): 498-505.

E. J. Murray. and James. D. Geddes., 1987. Uplift of anchor plates in sand. Journal of Geotechnical Engineering, **113** (3): 202-215.

Japan Geotechnical Society. 1995. Introduction Series **13**, Introduction to Soil Strength and Ground Destruction, 64.

Jin-yuan Liu., Ming-liang Liu. and Zhen-de Zhu., 2012. Sand deformation around an uplift plate anchor. Journal of Geotechnical and Geoenvironmental Engineering, **138** (6): 728-737.

Jaw-Guei Lin., S.-Y. Hsu. and San-Shyan S. Lin., 2015. The new method to evaluate the uplift capacity of belled piles in sandy soil. Journal of Marine Science and Technology, **23** (4): 523-533.

J. G. Kang., A. SHINJI. and N. YASUFUKU., 2018. Visual observation of the pull-out failure mode of belled-type pile in sandy soil and its evaluation. International Society of Offshore and Polar Engineers, 499-505.

K. Shanker., P. K. Basudhar. and N. R. Patra., 2007. Uplift capacity of single piles: predictions and performance. Geotechnical and Geological Engineering, **25** (2): 151-161.

K. Ilamparuthi., E. A. Dickin. and K. Muthukrisnaiah. 2002. Experimental investigation of the uplift behavior of circular plate anchors embedded in sand. Canadian Geotechnical Journal*,* **39** (3): 648-664.

Meyerhof, G, G., 1976. Bearing capacity and settlement of pile foundation. Journal of Geotechnical and Geoenvironmental Engineering*,* **102** (GT3): 197-228

M. MATSUO., 1967. Study on the uplift resistance of footing (I). Soils and Foundations, **7** (4): 1-37.

M. MATSUO., 1968. Study on the uplift resistance of footing (II). Soils and Foundations, **8** (1): 18-48.

M. UESUGI., H. KISHIDA. and Y. TSUBAKIHARA., 1988. Behavior of sand particles in sand-steel friction. Soils and Foundations, **28** (1): 107-118.

R. K. Rowe. and E. H. Davis., 1982. The behaviour of anchor plates in sand. Géotechnique, **32** (1): 25-41.

White. D. J., Cheuk. C. Y. and Bolton. M. D., 2008. The uplift resistance of pipes and plate anchors buried in sand. Géotechnique, **58** (10): 771-779.

W. P. Hong. and N. Chim., 2015. Prediction of uplift capacity of a micropile embedded in soil. KSCE Journal of Civil Engineering, **19** (1): 116-126.

Yoshio, H., Shuichi, W. and Masamichi, A. 2015. In-situ pull-out tests of cast-in-place concrete piles with belled enlargements. The 15th Asian Regional Conference on Soil Mechanics and Geotechnical Engineering. **2** (41): 1478-1481.

Tsuyoshi HONDA,Yoshio HIRAI. and Eiji SATO., 2011. Uplift capacity of belled and multi-belled piles in dense sand. Soils and Foundations, **51** (3): 483-496.

Acknowledgement

The authors express their gratitude to the laboratory technical assistant Mr. Michio Nakashima and laboratory member Mr. Jugdernamjil Amarbayar for their great support.

Symbols and abbreviations

A_b	Belled-type pile tip area
b_b	Diameter of belled-type pile tip
b_s	Diameter of pile shaft
b_e	Corrected diameter of pile tip
Dr	Relative density
θ_E	Pile tip failure surface
θ_i	Pile tip inclination angle
κ	Coefficient of unit weight
K_0, K_s	Coefficient of lateral earth pressure
K_u	Coefficient of uplift factor
L	Pile penetration depth
P_u	Ultimate uplift resistance
$P_{u(net)}$	Net ultimate uplift resistance
γ_d	Dry unit weight of sand
φ	Internal friction angle
ψ	Dilatancy angle ($\varphi/2°$, $\varphi - 30°$)
δ	Pile-soil friction angle ($\delta = \psi = \varphi/2°$)